Catalytic surface oxidation by rare-earth metals: A photoemission study of Gd- and Y-promoted oxidation of W(110)

R. I. R. Blyth,[1,2,*] C. Searle,[2] N. P. Tucker,[2] and S. D. Barrett[2]
[1]*National Nanotechnology Laboratory of INFM, Dipartimento di Ingegneria dell'Innovazione, Università di Lecce, Via Arnesano, 73100 Lecce, Italy*
[2]*Surface Science Research Centre and Department of Physics, University of Liverpool, Liverpool L69 3BX, United Kingdom*
(Received 23 March 2004; published 6 July 2004)

Catalytic oxidation of the substrate has been observed for rare-earth metals on refractory metal surfaces, where the mechanism responsible has been attributed to the ability of the rare earth to form oxides with more than one oxidation state. It has been postulated that, as a result, only rare earths with more than one oxidation state will exhibit catalytic activity, at least in terms of surface oxidation. We show, using high-resolution core-level photoemission, that submonolayer coverages of Gd and Y, two rare-earth metals with only one stable oxide each, promote catalytic oxidation of W(110). Initial oxygen dosing oxidizes the rare-earth overlayer, followed by oxidation of W(110) at higher rates, and with higher resulting oxidation states, than are observed for oxygen dosing on the clean surface. We suggest that the lowering of the W(110) work function, due to the presence of the rare-earth metals and/or their oxides, is responsible for the promoted oxidation. Catalytic activity of rare-earth metals is therefore not limited to those with more than one oxidation state.

DOI: 10.1103/PhysRevB.70.045402 PACS number(s): 79.60.Dp, 82.65.+r, 73.20.Hb

I. INTRODUCTION

Rare-earth-promoted oxidation of a surface was first observed two decades ago.[1] Using x-ray photoemission spectroscopy (XPS) of the Nb 3*d* level, Latta and Ronay observed[1] that Nb_2O_5 was formed on Nb with a thin Ce overlayer upon oxygen dosing, whereas the same oxygen dose on clean Nb produced only lower Nb oxides. They suggested that the Nb_2O_5 formation represented catalytic oxidation of the Nb substrate, following an initial oxidation of the Ce overlayer to Ce_2O_3, and proposed the following mechanism:

First, an oxygen molecule adsorbs and dissociates on a Ce_2O_3 unit. The Ce_2O_3 donates its two $4f^1$ electrons to an oxygen atom, which in turn occupies the oxygen-ion vacancy of the Ce_2O_3, oxidizing it to CeO_2

$$Ce_2O_3 + O \rightarrow 2CeO_2. \quad (1)$$

The two electron vacancies in the CeO_2 become subsequently occupied by electrons tunneling from the metallic substrate, thereby reducing the CeO_2 to Ce_2O_3

$$2CeO_2 + 2e^- \rightarrow Ce_2O_3 + O^{2-}. \quad (2)$$

This frees the O^{2-} ion to diffuse to the metal/oxide interface, where it readily reacts with the substrate, to form an oxide. Thus, the rate of uptake of oxygen is increased, and the energy barrier to higher oxide formation lowered. The process is discussed in considerably greater detail in Ref. 2. It is sufficient here to note that the process relies on the ability of Ce to form oxides with two different oxidation states.

This mechanism was further supported by the observation[3] that Ce, Pr, and Tb overlayers on Nb resulted in Nb_2O_5 production upon oxidation, whereas Er did not, the significance being that, of these rare earths, Er has only one possible oxidation state, while the others have two or more. These results have been taken as demonstrating that only rare earths with two (or more) oxidation states are catalysts,[4] at least from the perspective of surface oxidation. As a result, studies of rare-earth-promoted oxidation have focused on rare earths with multiple oxidation states.[4–11]

Latta and Ronay[3] used as their criterion for catalytic activity the formation of Nb_2O_5, and did not focus on the other aspect of catalytic oxidation, i.e., the possible increased rate of formation of lower oxides. Since rare earths with single oxidation states have been ignored in the literature on catalytic oxidation of surfaces, it is not known whether these metals are also capable of promoting higher oxidation rates, i.e., of displaying catalytic activity. In this work we study the oxidation-promotion capabilities of the rare earth metals Y and Gd. For both these metals only the sesquioxide (RE_2O_3) is known,[12] since the ability to form higher oxidation states by donating a 4*f* electron into the valence band *d* shell is clearly absent in Y, and greatly hindered by the stability of the half-full 4*f* shell in Gd.

Refractory metal surfaces, such as that of Nb studied by Latta and Ronay[1–3] are, in general, particularly suited to studies of catalytic oxidation by rare earths. Studies of rare-earth-promoted oxidation of other surfaces, such as Si[5–7] and Al,[8,9,13,14] have been performed, but on these surfaces there is a certain degree of rare-earth intermixing with the substrate. On refractory metals, in contrast, rare earths do not form surface alloys upon adsorption.[1,2,4,10] However, the 3*d* levels of Nb are not particularly suited to the study of lower oxide formation, as the resulting chemical shifts are of the same order as the photoemission linewidth.[15,16] For high-resolution photoemission studies of rare-earth catalyzed oxidation, Ta and W have been used as substrates. Here, the sharp 4*f* lines, with linewidths of the order of 100 meV (for the W $4f_{7/2}$ level,[17] for example) allow the clear identification of lower oxidation states.[4,10,18] Ce-catalyzed oxidation of Ta(110)[10] and W(110)[4] and W(111)[4] has previously been investigated, with higher oxide formation observed for Ce/W(111)[4] and

Ce/Ta(110).[10] The case of Ce on W(110) is of particular interest, since here the catalytic oxidation was inferred entirely from the increased rate of production of the two-dimensional WO that forms on W(110).[4] Oxidation states higher than WO are unknown on W(110),[17] as it appears oxygen is unable to penetrate the surface to form bulk oxides. We therefore chose to investigate Y and Gd on W(110), since here a direct comparison with a Ce-catalyzed system showing no higher oxide formation is possible. Further, the possible oxygen absorption sites and their corresponding W $4f$ binding energy shifts for oxygen on clean W(110) have been thoroughly investigated,[18] greatly aiding the interpretation of photoemission data. We concentrate on the behavior of oxygen on Y precoated W(110), since here there can be absolutely no question that the mechanism of Latte and Ronay is possible. Note that similar behavior is to be expected for Gd, since although Y is very much lighter, it is often grouped, from the point of view of chemical behavior, with the heavy lanthanides (i.e., Gd-Lu). Indeed, band structure calculations[19] show that the electronic structure of Y is very similar to that of Gd.[20] Further, core-level photoemission spectroscopy shows essentially identical behavior of Y and Gd on W(110).[21]

II. EXPERIMENT

The experiments were performed on beamline 4.1,[22] at the Synchrotron Radiation Source, Daresbury Laboratory, U.K., using a Vacuum Science Workshop HA54 angle-resolved analyzer in a vacuum chamber with a base pressure $<10^{-10}$ mbar. All spectra were recorded at an emission angle of 35°, using p-polarized light, incident at 5°. For W $4f$ spectra, photon energies of 70 and 100 eV were used, with overall energy resolutions (beamline plus analyzer) of 190 and 300 meV, respectively. The W(110) sample was cut from a commercially obtained boule with a purity >99.99% and subsequently polished to within 1° of the (110) face. *In situ* cleaning was achieved by heating the sample to 1500 K in 10^{-6} mbar of O_2 for 60 min, followed by repeated flashing to 2300 K. Surface order and cleanliness were monitored by low-energy electron diffraction, and photoemission of the W $4f$ core level, which is known to be sensitive to contamination.[17] Gd and Y were evaporated from a water-cooled tungsten wire basket evaporator, which was extensively outgassed prior to deposition. Approximately half-monolayer coverages of Y and Gd on W(110), hereafter Y/W(110) and Gd/W(110), respectively, were prepared, with the coverages estimated by comparison with the W $4f_{7/2}$ photoemission spectra of Tucker *et al.*[21] O_2 (99.997% pure) was obtained from Gas Distillers, and was dosed by background exposure, with the purity checked by mass spectrometer, and the quoted dosages derived from uncorrected ion gauge readings. All rare-earth deposition and photoemission measurements were performed at room temperature. Oxygen dosing was performed at room temperature except where stated.

III. RESULTS AND DISCUSSION

Photoemission spectra of the W $4f$ and $5p_{3/2}$ peaks, taken using a photon energy of 100 eV to enable a direct comparison with the data of Gu *et al.*,[4] are shown in Fig. 1. The $4f$ peaks of the clean surface show a shoulder to lower binding energy due to the well-known W(110) surface core-level shift.[17] This shift is of the order of 0.3 eV,[17] and is not resolved in these data. Upon oxygen dosing, the surface peak disappears and a broad shoulder to lower binding energy forms, corresponding to a $p(2\times1)$ overlayer structure.[18,23] The highest coverage obtainable at room temperature is a half-monolayer,[18] corresponding to the spectrum of clean W(110) with a 20 L dose in Fig. 1. Higher coverages can be obtained by dosing at elevated temperatures,[18] and Fig. 1 shows the spectrum resulting from a very high dose at 1500 K. This spectrum clearly shows a peak at a binding energy ~0.6 eV higher than that of the bulk peak, attributed to the formation of two-dimensional WO.[4,18] The WO peak is visible only as a weak shoulder in the spectrum obtained after room temperature dosing. A clear WO peak is also visible in the spectrum of oxygen-dosed Ce/W(110) of Gu *et al.*[4] in Fig. 1. The presence of this peak, rather than a weak shoulder, after (room temperature) oxygen dosing on the Ce-precoated surface, was taken by Gu *et al.* as evidence for the catalytic oxidation of W(110) by Ce.[4] They suggested that the valence-change mechanism of Latta and Ronay was responsible for this catalytic oxidation. However, Fig. 1 shows that the WO peak is also obtained when dosing oxygen on Y/W(110) and Gd/W(110).

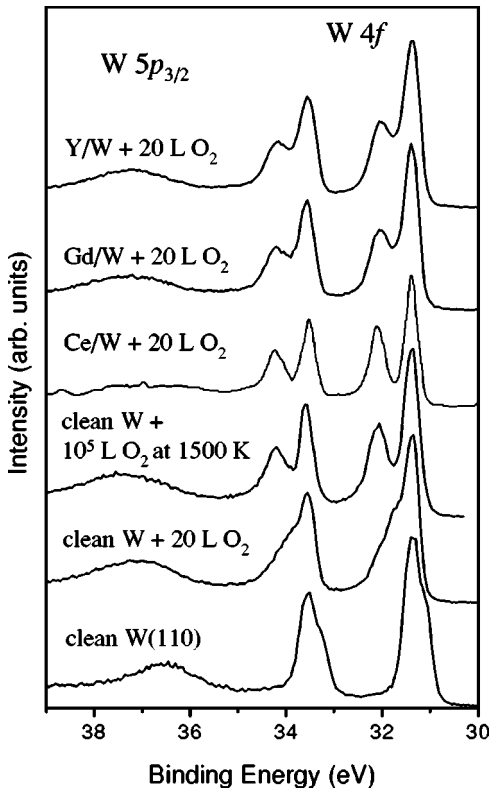

FIG. 1. Photoemission spectra ($h\nu$=100 eV) of the W $4f$ and $5p_{3/2}$ core levels of clean W(110), clean W(110) exposed to oxygen, W(110) roasted (1500 K) in 10^{-6} mbar O_2 for 1 h, and W(110) with half-monolayer coverages of Gd and Y exposed to oxygen. Also shown is the spectrum of Ce-precoated W(110) exposed to oxygen from Ref. 4, which was taken using $h\nu$=110 eV.

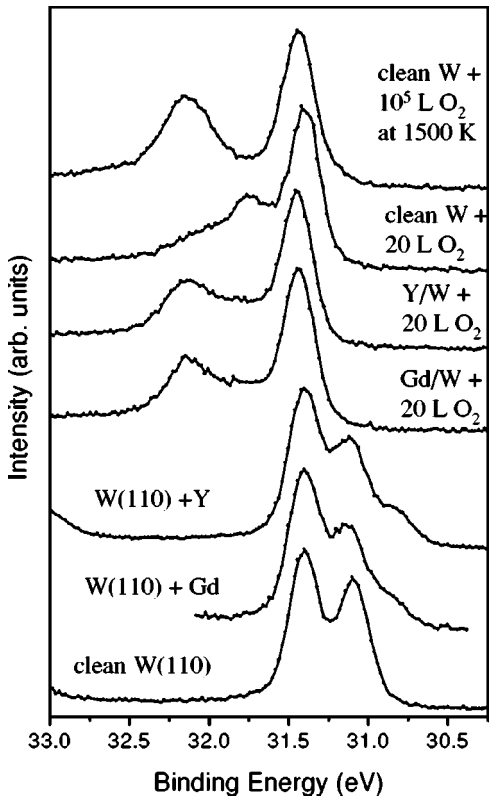

FIG. 2. Photoemission spectra ($h\nu$=70 eV) of the W $4f_{7/2}$ core level of clean W(110), W(110) with half-monolayer coverages of Gd and Y, the rare-earth pre-covered W(110) surfaces after exposure to oxygen, clean W(110) exposed to oxygen, and W(110) roasted (1500 K) in 10^{-6} mbar O_2 for 1 h.

Higher resolution W $4f_{7/2}$ data are shown in Fig. 2. Here, the surface shift of the clean surface is clearly resolved, while spectra of Y/W(110) and Gd/W(110) show a surface peak reduced in intensity, with a further shoulder at even lower binding energy. This peak is attributed[21,24] to the series of $(n\times 2)$ structures that rare earths form at submonolayer coverages on W(110).[25] For oxygen dosing on clean W(110) the shoulder at lower binding energy seen in Fig. 1 is now resolved as a peak with a shift of 0.3 eV, due to $p(2\times 1)$-O,[18] with a shoulder at ~0.6 eV, due to WO.[18] The high temperature dose shows the WO peak now well-resolved, with a well-formed valley between the bulk and WO peaks. For Y/W(110) and Gd/W(110), oxygen dosing appears to produce a situation intermediate to the room temperature and high temperature results from the clean surface, i.e., a greater production of WO compared to the room temperature dose, but retaining a higher proportion of $p(2\times 1)$-O than the high temperature dose.

A series of W $4f_{7/2}$ photoemission spectra of Y/W(110), exposed to increasing doses of oxygen, is shown in Fig. 3. Initially, the only obvious change is the loss of the rare-earth-induced shoulder at low binding energy. Once this peak can no longer be readily distingushed the surface peak also starts to lose intensity, while the $p(2\times 1)$ shoulder gains in intensity. At higher doses the surface peak can no longer be seen, while the unresolved WO and $p(2\times 1)$ peaks increase in intensity.

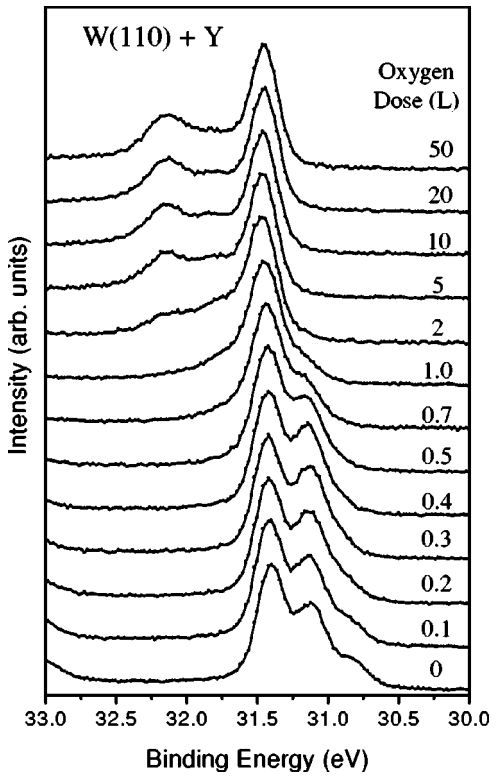

FIG. 3. Photoemission spectra ($h\nu$=70 eV) of the W $4f_{7/2}$ core level of W(110) with a half-monolayer coverage of Y, exposed to increasing doses of O_2.

In order to extract quantitative information from the spectra of Fig. 3, we analyzed the data using a nonlinear least-squares fitting procedure. The W $4f_{7/2}$ binding energies for the possible W-O coordinations for oxygen on W(110) have been determined, using high-resolution photoemission, by Riffe and Wertheim,[18] considering the structures observed by STM.[23] The possible adsorption sites are shown in Fig. 4. As the W(110) surface is not close-packed, there are no simple threefold symmetric hollow sites. Rather, the adsorption site lies at one end of the "hourglass" depressions between W

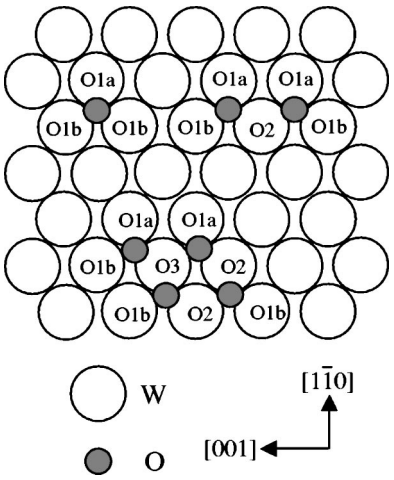

FIG. 4. Schematic diagram of the chemically distinct types of surface W atoms for oxygen on W(110).

TABLE I. *W* $4f_{7/2}$ binding energies and peak assignments.

Binding energy (eV)	Shift (eV)	Assignment	Ref.
31.4	—	Bulk (B)	17
31.1	−0.3	Clean surface (S)	17
30.8	−0.6	RE($n\times2$)	21 and 24
31.24	−0.16	O1a	18
31.48	+0.08	O1b	18
31.8	+0.4	O2	18
32.1	+0.7	O3	18
32.7	+1.3	O4	This work

neighbors in the [001] direction. Thus, isolated oxygen atoms give rise to two distinct W surface species, O1a, corresponding to W atoms at the "top" of the hourglass, and O1b corresponding to W atoms at the side of the hourglass. Twofold coordinated W atoms are designated O2, while threefold coordination is designated O3. Note that the O3 species corresponds to an overlayer with a W:O surface stochiometry of 1:1, hence is referred to as two-dimensional WO, as bulk WO is not well known.[26] The possible W species and their corresponding W $4f_{7/2}$ binding energies are summarized in Table I.

For curve fitting, we used the standard line shape for metallic core levels, i.e., a Doniach-Sunjic line shape[27] convoluted with a Gaussian function representing instrumental and inhomogeneous broadening, as used by Riffe and Wertheim in their high-resolution study of oxygen on W(110),[18] and Tucker *et al.*[21] in their study of rare earths on W(110). The Doniach-Sunjic line shape[27] includes a Lorentzian component representing the lifetime width of the peak, and a singularity index which defines the asymmetric high-binding-energy tail of the photoemission peak of a metallic surface. We used a linear background, as used by Riffe and Wertheim[18] and Tucker *et al.*[21] The parameters for the bulk, surface, and rare-earth ($n\times2$) peaks were taken from the fit to the spectrum obtained before oxygen dosing.

For oxygen doses up to 0.5 L, as shown for selected spectra in Fig. 5, only bulk, surface, and rare-earth peaks were required to give a good fit. Note that the tailing off of the residuals in Fig. 5 at higher binding energy is due to the presence of a contribution to the background from the W $4f_{5/2}$ peak, which was not considered in the fitting process.

For the spectrum following an oxygen dose of 0.7 L, Fig. 6, further peaks were required to give a good fit. While the number of oxygen-induced peaks in Table I may seem excessive, particularly when they are not clearly resolved, Riffe and Wertheim[18] have shown convincingly that this number is in fact required. We also attempted to fit the 0.7 L spectrum using only one peak to represent the adsorbed oxygen, but, as Fig. 6(a) shows, we could not obtain a good fit, even when allowing totally unconstrained parameters—note in particular the highly unphysical asymmetry of the surface component. Riffe and Wertheim[18] further note that since they restrained their fits such that the oxygen-induced peaks shared

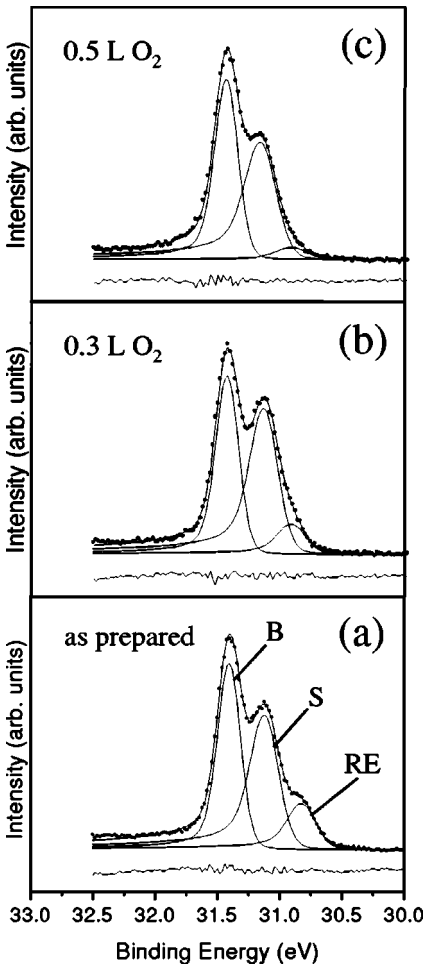

FIG. 5. Photoemission spectra ($h\nu$=70 eV) of the W $4f_{7/2}$ core level of W(110) with a half-monolayer coverage of Y, and exposed to doses of 0.3 and 0.5 L O_2. Also shown are the results of the fitting procedure. See the text for details.

the Lorentzian width and asymmetry of the surface peak, a practice we also followed, the six-component fit (B, S, O1a, O1b, O2, O3) actually has fewer parameters than an unrestrained three-component (B, S, O) fit such as that in Fig. 6(a). For the surface peaks (clean and oxygen-coordinated) components, we used the binding energies of Riffe and Wertheim, with the Lorentzian widths and asymmetries of the oxygen-coordinated peaks constrained to be those of the surface peak. Figure 6(b) shows that this gives a good fit, again excepting the background where the W $4f_{5/2}$ peak interferes. For this dose, an O3 peak was not required to give a good fit, but the inclusion of this peak was required at higher coverages. For the spectra at higher coverages the parameters of the oxygen-induced peaks, except intensity, were kept constant, which also produced good fits, as shown in Fig. 7. We found that the binding energy of the bulk peak shifted very slightly to higher binding energies with oxygen dose, with the total shift being 20 meV, but no relaxation of the other peak binding energies with dose was required. In addition, for the higher doses, we found that a further small component was required at higher binding energy. Riffe and Wertheim noted a similar peak in their data for Cs-promoted

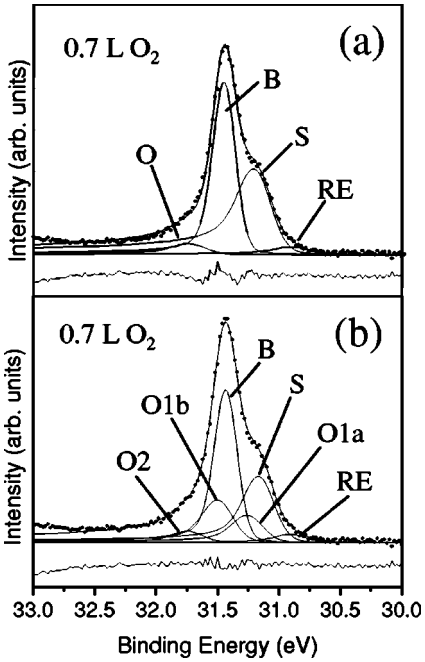

FIG. 6. Photoemission spectra ($h\nu$=70 eV) of the W $4f_{7/2}$ core level of W(110) with a half-monolayer coverage of Y, exposed to a dose of 0.7 L O_2. Also shown are the results of the fitting procedure using (a) only one oxygen-induced peak (O2) and (b) three oxygen-induced peaks (O1a, O1b, and O2).

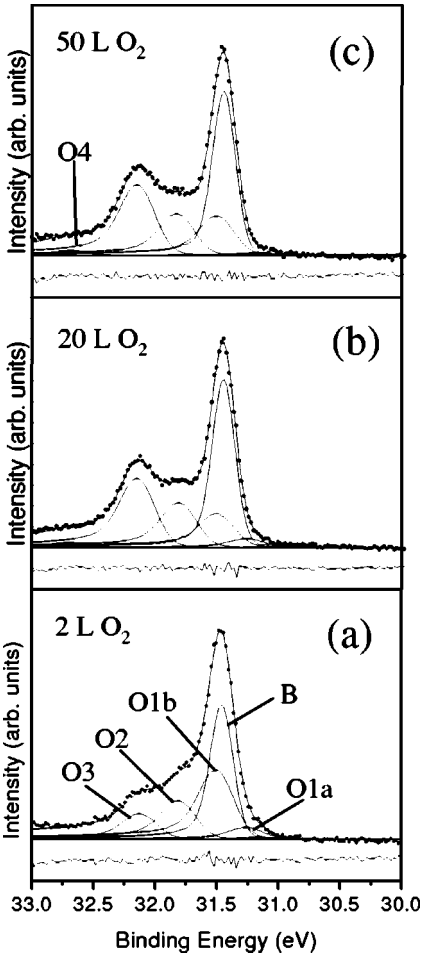

FIG. 7. Photoemission spectra ($h\nu$=70 eV) of the W $4f_{7/2}$ core level of W(110) with a half-monolayer coverage of Y, exposed to doses of 2, 20, and 50 L O_2. Also shown are the results of the fitting procedure.

oxidation of W(110),[18] which they attributed to bridge-bonded oxygen, which would give a possible fourfold coordination of the W atoms. In the data of Riffe and Wertheim this peak was less well-resolved than in our data; therefore, we did not regard their binding energy as definitive, and in fact we find this peak at a rather higher binding energy. This peak is designated O4 in Fig. 7(b).

The intensities of the various components of the W $4f_{7/2}$ peak, determined from fits such as those in Figs. 5–7, are shown in Fig. 8. Initially it can be seen that the surface appears to be getting cleaner—the RE peak intensity is reducing while that of the clean surface is increasing. It therefore appears that in the initial stage of the oxidation process the yttrium, and not the tungsten, is being oxidized. The RE peak in the W $4f$ spectra is thought to be due to charge transfer from the rare-earth adsorbate to the tungsten substrate.[21] With the Y oxidized to Y_2O_3, an ionic solid with an empty Y valence band, this charge transfer can no longer occur, restoring the surface binding energy to its initial value. If there is a small shift, relative to the true clean surface, due to the presence of a surface yttrium oxide species, it is not resolved in our data. Therefore, we have chosen not to incorporate a further species in the fit. The continued presence of Y atoms on the surface is relatively difficult to confirm using photoemission, as of course yttrium has no sharp, intense, $4f$ levels. With the Y $3d$ peak inaccessible on the beamline used, the most intense Y core levels available were the $4p$ levels. The cross section of the Y $4p$ levels is an order of magnitude less than the rare-earth $4f$ levels at $h\nu$=70 eV.[28] Further, the Y $4p$ levels are in the same binding energy region as the O $2s$ level, which has a cross section a factor of 2 higher than the Y $4p$ levels at $h\nu$=70 eV.[28] However, we can use the $4f$ levels of Gd to determine the presence of the rare earth after the oxidation process. Figure 9(a) shows the spectrum of Gd/W(110) before oxygen dosing, with the Gd $4f$ visible as the peak at 8.5 eV binding energy.[29,30] After oxidation, Fig. 9(b), the $4f$ peak can no longer be clearly distinguished—there is some structure in the region 6–8 eV, but this is also where the O $2p$ level would be expected.[18] The Gd contribution can be extracted using resonant photoemission. At a photon energy of 150 eV, there is a coincidence of the Gd $4d$-$4f$ resonance and the W $5d$ Cooper minimum,[31] while the cross section of the O $2p$ level has decreased by a factor of 5 from $h\nu$=70 eV.[28] Figure 9(c) shows the spectrum at this photon energy. Here, the Gd $4f$ is now clearly present, and can be identified as the peak at 7.5 eV in the spectrum of Fig. 9(b). The $4f$ peak of Fig. 9(c) shows the broad line shape characteristic of rare-earth ionic solids,[32] but it has a binding energy lower than the metallic Gd $4f$, not the higher binding energy, 9.6 eV,[33] expected for Gd_2O_3. This apparent anomaly can be understood by considering the band-alignment models of Fig. 10. Figure 10(a) shows the situation for metallic Gd on W(110). Here there is charge transfer, so the Fermi levels align and the Gd $4f$ ap-

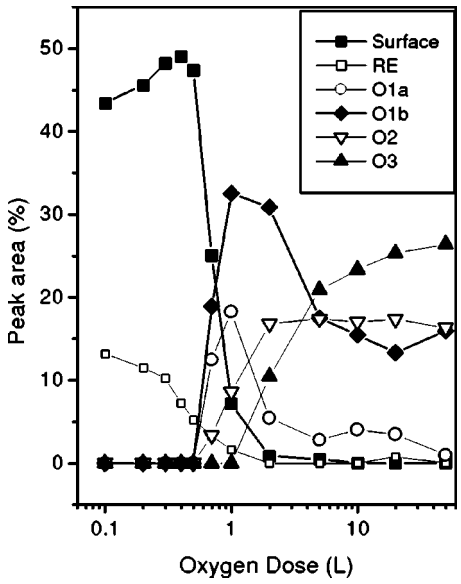

FIG. 8. Percentage contributions of the surface-related components of the curve fits of Figs. 4–6 to the overall line shape.

pears at its metallic binding energy relative to the W, and hence spectrometer, Fermi level. The data of Figs. 3 and 5 suggest that there is no charge transfer to or from the W substrate, as the surface W 4*f* binding energy after initial oxidation is the same as that of clean W(110). Therefore, a vacuum level alignment model is appropriate, as shown in Fig. 10(b). Here, the low work function of rare-earth sesquioxides, ~2 eV,[34] compared to the 5.25 eV of W(110),[35] ensures that the shift to higher binding energy of the Gd 4*f* upon oxidation is more than offset by the difference in work functions.

The practical result of this initial rare-earth oxidation is that at low oxygen doses the W itself is not oxidized—not until the RE peak has lost most of its intensity is there significant coverage of oxygen-coordinated tungsten. In Fig. 8, the O1a component reaches a maximum, and then decreases,

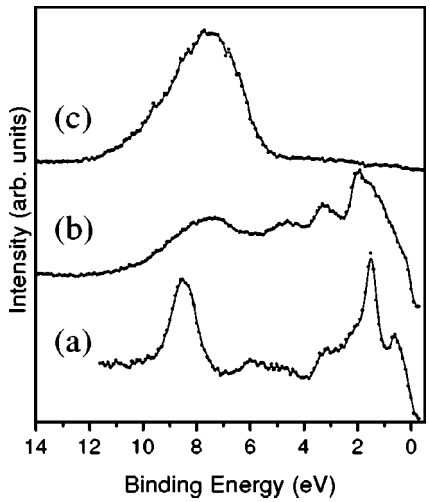

FIG. 9. Photoemission spectra of (a) half-monolayer coverage of Gd on W(110), $h\nu$=70 eV; (b) the same surface exposed to 20 L O_2, $h\nu$=70 eV; (c) as (b) except $h\nu$=150 eV.

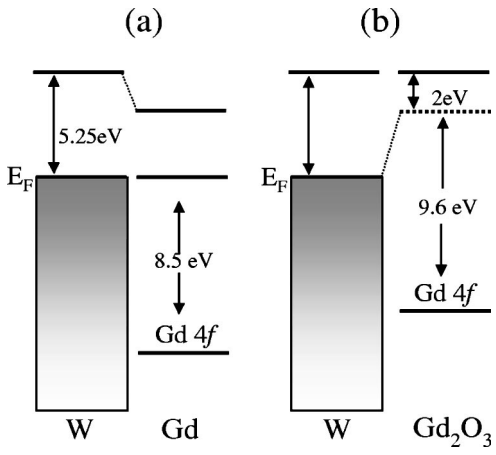

FIG. 10. Band alignment models for the photoemission spectra of Fig. 9.

while the O2 peak increases steadily. This is also seen for dosing on clean W(110),[18] but in all other respects the data are very different. In Fig. 8 the O1b component also reaches a maximum and then decreases, while O2 formation reaches a saturation level long before oxidation is complete. Both these components increase fairly linearly towards saturation on clean W(110).[18] A further significant difference is that O3 formation begins very quickly after the O1a and O1b components appear, whereas on clean W(110) there is no significant O3 formation until near saturation.[18]

For comparison with the curve-fit results for oxygen on Y/W(110), curve fits, using the same parameter set, were also perfomed for the spectra of oxygen on clean W(110) and Gd/W(110) of Fig. 2. The results of these fits are shown in Fig. 11, with the percentage contributions of each component to the overall line shape summarized in Table II.

The sum of the contributions of the O1a and O1b peaks, i.e., the singly coordinated W surface atoms, to the overall line shape is similar for all four substrates. The principal difference is the balance between the O2 and O3 contributions, with the presence of the RE overlayer selectively favoring the production of O3 sites over O2.

A visual inspection of the data of Figs. 2 and 11 suggests that the oxygen coverage on RE/W(110) is significantly greater than for a similar oxygen dose on clean W(110). The fits of Figs. 7 and 11 permit a more quantitative analysis. By considering the fractional intensities of the surface-related (i.e., clean and oxygen-coordinated) peaks, F_s, the absolute oxygen coverage (in ML), θ, can be calculated using[18]

$$\theta = \frac{\Sigma_s \frac{n_O F_s}{n_W}}{\Sigma_s F_s}, \tag{3}$$

where n_O is the number of oxygen atoms that coordinate the W atom associated with a given peak, and n_W is the coordination number of the W atoms (which is always 3). For the clean surface peak, n_O=0 (however, in all cases the intensity of the surface peak was zero). For peaks O1a and O1b, n_O =1, for peak O2, n_O=2, for peak O3, n_O=3, and for peak

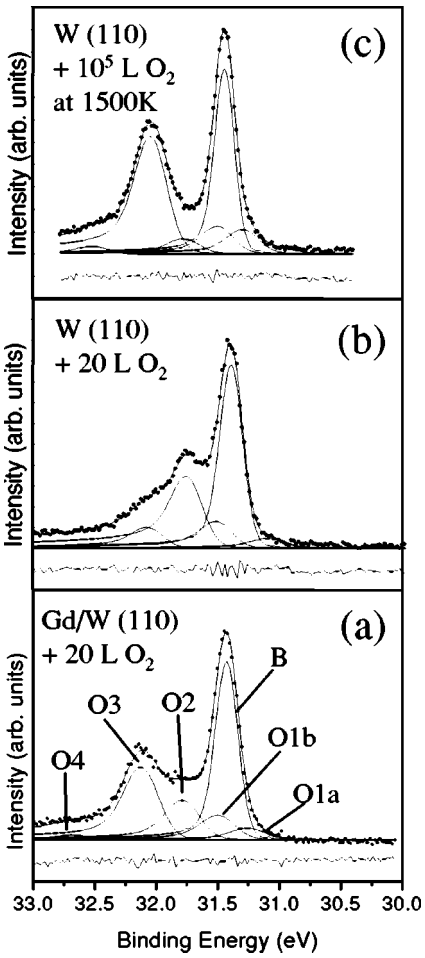

FIG. 11. Photoemission spectra ($h\nu$=70 eV) of the W $4f_{7/2}$ core level of (a) W(110) with a half-monolayer coverage of Gd, exposed to 20 L O_2; (b) clean W(110) exposed to 20 L O_2, and (c) clean W(110) roasted (1500 K) in 10^{-6} mbar O_2 for 1 h (10^5 L). Also shown are the results of the fitting procedure.

O4, n_O=4. The results are shown in Table III. Note that the room temperature dose has produced a coverage slightly higher than the 0.5 monolayer obtained by Riffe and Wertheim.[18] In comparison with their data we obtain a slightly higher O3 coverage, which may reflect a slightly higher defect density on our crystal. For the RE/W(110) substrates, the overall coverage is ~0.75 monolayer, a significant increase compared to the clean W(110) result, and

TABLE II. Percentage contributions of each peak.

Peak	W(110)/Y +20 L O_2	W(110)/Gd +20 L O_2	W(110) +20 L O_2	W(110) +10^5 L O_2 (1500 K)
O1a	3.5	5.0	4.6	8.6
O1b	13.3	10.0	12.0	9.5
O2	17.3	15.6	30.7	5.1
O3	25.3	27.0	8.4	37.5
O4	1.6	1.6	0	2.0

TABLE III. Absolute oxygen coverages, θ.

W(110)/Y +20 L O_2	W(110)/Gd +20 L O_2	W(110) +20 L O_2	W(110) +10^5 L O_2 (1500 K)
0.70	0.74	0.60	0.77

not far short of the coverage produced by high temperature dosing on clean W(110).

Since the oxidation state exchange mechanism of Latta and Ronay[1] cannot be occurring for Y or Gd, it follows that some other mechanism must be responsible for the promoted oxidation. The results of Fig. 2 are very similar to those of Riffe and Wertheim, who noted in passing that alkali metals promoted the oxidation of W(110),[18] which suggests that a common mechanism may be responsible. While redox reactions such as those of Eqs. (1) and (2) can promote oxidation, a simple lowering of the work function may also suffice, as has been noted for K-promoted oxidation of Ta,[36] for example, and also for promoted oxidation of mixed rare-earth/Al surfaces.[13,14] The rate-limiting step for oxidation is generally that of the dissociation of the O_2 molecule. This proceeds via the population of an O_2 π^* antibonding state via electron transfer from the surface. Lowering the work function, which is equivalent to raising the Fermi level, greatly facilitates this mechanism, as is shown nicely, for example, in the calculations of Sjövall *et al.*[37] for K-promoted oxidation of graphite. The work function of W(110) is dramatically lowered by alkali-metal adsorption—for example, from 5.25 eV for clean W(110)[35] to as low as 1.5 eV for a half-monolayer coverage of Cs.[38,39] Rare-earth metals also lower the work function of W(110),[40] and rare-earth oxide work functions are also relatively low, at around 2 eV.[34] Rare-earth metal (0001) surfaces, with work functions ~3 eV, have been shown to be capable of dissociating a wide range of molecules,[41] including oxygen.[42]

IV. CONCLUSIONS

At low oxygen doses on rare-earth precoated W(110) surfaces the rare earth oxidizes preferentially, with tungsten oxidation proceeding after this process is essentially complete. These observations shed some light onto a recent anomaly in the literature regarding rare-earth catalysis. Although both Ce and Pr were found to catalytically oxidize Nb,[1,2] in a recent study[11] Hwang found that Pr did not catalytically oxidize W(110). However, that study was limited to relatively low doses of oxygen, where our data suggest that oxidation of the W substrate would not have begun. The data of Hwang are therefore not inconsistent with catalytic activity of Pr.

Both Y and Gd have been shown to catalytically oxidize W(110). In both cases the presence of rare-earth atoms results in the selective favoring of triply coordinated tungsten over doubly coordinated tungsten at saturation, with a corresponding increase of the absolute oxygen coverage. Therefore, catalytic activity of rare-earth metals in surface oxidation is not limited to those rare earths with multiple oxidation

states. In hindsight, this perhaps should not come as a surprise, since catalytic activity of rare-earth oxides, including those of Y and Gd, is not unknown.[43] Further, the results for Gd/W(110)) and Y/W(110) can be seen in Figs. 1 and 2 to be extremely similar to those for Ce/W(110),[4] suggesting that the mechanism of Latta and Ronay need not be invoked even in cases where it is possible. We suggest that the simple act of lowering the W(110) work function, by rare earths and/or rare-earth oxides, may be sufficient to promote oxidation. The extent of the rare-earth-promoted oxidation on W(110) is considerably less than that promoted by Ce on more open surfaces;[4,10] therefore, it remains to be seen whether rare earths with single oxidation states are capable of promoting oxidation to the same level as those with multiple oxidation states, in cases where higher oxidation is possible.

ACKNOWLEDGMENTS

We would like to thank Andy Robinson for assistance at DL, and the UK EPSRC for funding.

*Electronic address: rob.blyth@unile.it

[1] E. E. Latta and M. Ronay, Phys. Rev. Lett. **53**, 948 (1984).
[2] M. Ronay and E. E. Latta, Phys. Rev. B **32**, 5375 (1985).
[3] E. E. Latta and M. Ronay, J. Vac. Sci. Technol. A **4**, 1626 (1986).
[4] C. Gu, C. G. Olson, and D. W. Lynch, Phys. Rev. B **48**, 12178 (1993).
[5] F. U. Hillebrecht, M. Ronay, D. Rieger, and F. J. Himpsel, Phys. Rev. B **34**, 5377 (1986).
[6] S. Chang, P. Philip, A. Wall, A. Raisanen, N. Troullier, and A. Franciosi, Phys. Rev. B **35**, 3013 (1987).
[7] J. Onsgaard, J. Ghijsen, R. L. Johnson, M. Christiansen, F. Orskov, and P. J. Godowski, Phys. Rev. B **43**, 4216 (1991).
[8] N. A. Braaten, J. K. Grepstad, and S. Raaen, Surf. Sci. **222**, 499 (1989).
[9] S. Raaen and N. A. Braaten, Phys. Rev. B **41**, 12270 (1990).
[10] C. Gu, D. W. Lynch, A. B. Yang, and C. G. Olson, Phys. Rev. B **42**, 1526 (1990).
[11] C. Hwang, Surf. Sci. **385**, 328 (1997).
[12] G.-Y. Adachi and N. Imanaka, Chem. Rev. (Washington, D.C.) **98**, 1479 (1998).
[13] C. Berg, S. Raaen, and A. Borg, Surf. Sci. **303**, 114 (1994).
[14] F. Strisland and S. Raaen, J. Electron Spectrosc. Relat. Phenom. **77**, 25 (1996).
[15] M. Grundner and J. Halbritter, J. Appl. Phys. **51**, 397 (1980).
[16] A. Arfaoui, C. Gouillot, J. Cousty, and C. Antoine, J. Appl. Phys. **91**, 9319 (2002).
[17] D. M. Riffe, G. K. Wertheim, and P. H. Citrin, Phys. Rev. Lett. **63**, 1976 (1989).
[18] D. M. Riffe and G. K. Wertheim, Surf. Sci. **399**, 248 (1998).
[19] P. Blaha, K. Schwarz, and P. H. Dederichs, Phys. Rev. B **38**, 9368 (1988).
[20] R. Wu, C. Li, A. J. Freeman, and C. L. Fu, Phys. Rev. B **44**, 9400 (1991).
[21] N. P. Tucker, R. I. R. Blyth, R. G. White, M. H. Lee, C. Searle, and S. D. Barrett, J. Phys.: Condens. Matter **10**, 6677 (1998).
[22] V. R. Dhanak, A. W. Robinson, G. van der Laan, and G. Thornton, Rev. Sci. Instrum. **63**, 1342 (1992).
[23] K. E. Johnson, R. J. Wilson, and S. Chiang, Phys. Rev. Lett. **71**, 1055 (1993).
[24] R. G. White, R. I. R. Blyth, N. P. Tucker, M. H. Lee, and S. D. Barrett, J. Synchrotron Radiat. **2**, 261 (1995).
[25] S. D. Barrett and S. S. Dhesi, *The Structure of Rare-Earth Metal Surfaces* (Imperial College Press, London, 2001).
[26] *Gmelin Handbuch der Anorganischen Chemie*, System No. 54, Wolfram B2 (Springer, Berlin, 1979), p. 14.
[27] S. Doniach and M. Sunjic, J. Phys. C **3**, 285 (1970).
[28] J. J. Yeh and I. Lindau, At. Data Nucl. Data Tables **32**, 1 (1985).
[29] J. K. Lang, Y. Baer, and P. A. Cox, J. Phys. F: Met. Phys. **11**, 121 (1981).
[30] A. V. Fedorov, E. Arenholz, K. Starke, E. Navas, L. Baumgarten, C. Laubschat, and G. Kaindl, Phys. Rev. Lett. **73**, 601 (1994).
[31] N. P. Tucker, R. I. R. Blyth, M. H. Lee, A. W. Robinson, and S. D. Barrett, J. Synchrotron Radiat. **2**, 252 (1995).
[32] C. W. Thiel, H. Cruguel, H. Wu, Y. Sun, G. J. Lapeyre, R. L. Cone, R. W. Equall, and R. M. Macfarlane, Phys. Rev. B **64**, 085107 (2001).
[33] D. Raiser and J.-P. Deville, J. Electron Spectrosc. Relat. Phenom. **57**, 91 (1991).
[34] K. Koumoto, W. S. Seo, and S. Oszawa, Appl. Phys. Lett. **71**, 1475 (1997).
[35] R. A. Strayer, W. Mackie, and L. W. Swanson, Surf. Sci. **34**, 225 (1973).
[36] N. A. Braaten, J. K. Grepstad, and S. Raaen, Surf. Sci. **250**, 51 (1991).
[37] P. Sjövall, B. Hellsing, K.-E. Keck, and B. Kasemo, J. Vac. Sci. Technol. A **5**, 1065 (1987).
[38] J. N. M. van Wunnik, J. J. C. Geerlings, and J. Los, Surf. Sci. **131**, 1 (1983).
[39] J. J. C. Geerlings, P. W. van Amersfoort, L. F. T. Kwakman, E. H. A. Granneman, and J. Los, Surf. Sci. **157**, 151 (1985).
[40] J. Kolaczkiewicz and E. Bauer, Surf. Sci. **175**, 487 (1986).
[41] R. I. R. Blyth, C. Searle, N. P. Tucker, R. G. White, T. K. Johal, J. Thompson, and S. D. Barrett, Phys. Rev. B **68**, 205404 (2003).
[42] E. Vescovo, O. Rader, T. Kachel, U. Alkemper, and C. Carbone, Phys. Rev. B **47**, 13899 (1993).
[43] For a review of rare-earth oxides and their catalytic behavior see G. A. M. Hussein, J. Anal. Appl. Pyrolysis **36**, 111 (1996).